Buffer-Aided Relay Selection for Cooperative NOMA in the Internet of Things

Mohammad Alkhawatrah, Yu Gong, Gaojie Chen, *Senior Member, IEEE*,
Sangarapillai Lambotharan, *Senior Member, IEEE*, and Jonathon A. Chambers, *Fellow, IEEE*

***Abstract*—The non-orthogonal multiple access (NOMA) well improves the spectrum efficiency which is particularly essential in the Internet of Things (IoT) system involving massive number of connections. It has been shown that applying buffers at relays can further increase the throughput in the NOMA relay network. This is however valid only when the channel signal-to-noise ratios (SNR-s) are large enough to support the NOMA transmission. While it would be straightforward for the cooperative network to switch between the NOMA and the traditional orthogonal multiple access (OMA) transmission modes based on the channel SNR-s, the best potential throughput would not be achieved. In this paper, we propose a novel prioritization-based buffer-aided relay selection scheme which is able to seamlessly combine the NOMA and OMA transmission in the relay network. The analytical expression of average throughput of the proposed scheme is successfully derived. The proposed scheme significantly improves the data throughput at both low and high SNR ranges, making it an attractive scheme for cooperative NOMA in the IoT.**

***Index Terms*—NOMA, Buffer-aided relay selection, cooperative network, throughput *l*th**

I. Introduction

The Internet of Things (IoT) aims at connecting massive number of devices, imposing great challenges in mobile network design [1], [2]. The non-orthogonal multiple access (NOMA), which improves transmission efficiency by allowing multiple devices share the same spectrum resources [3]–[7], provides an attractive solution to achieve massive connectivity in the IoT [8]–[10]. The NOMA has been successfully applied in cooperative relay selection networks. In [11], a two-stage relay selection scheme is described to maximize the throughput for one NOMA user upon satisfying the target transmission for the other. Other examples include a joint user and relay selection technique in the cooperative NOMA network [12], and a dual NOMA relay selection scheme with space time coding [13]. On the other hand, another recent development in cooperative networks is to apply data buffers at the relays [14]–[17], in which the transmission can be better aligned with strong links than traditional schemes such as the *max-min* relay selection [18]. Buffer-aided relay schemes have been applied in various applications including physical layer security [19], device-to-device communications [20] and cognitive radio networks [21].

This work was supported by EPSRC grant number EP/R006377/1 ("M3NETs").

M. Alkhawatrah, Y. Gong and S. Lambotharan are with Wolfson School of Mechanical, Electrical and Manufacturing Engineering, Loughborough University, UK, Email: {m.alkhawatrah, y.gong and s.lambotharan}@lboro.ac.uk.

G. Chen and J. A. Chambers are with the Department of Engineering, University of Leicester, UK, Emails: {gaojie.chen and jonathon.chambers}@leicester.ac.uk

Buffer techniques have been applied in the NOMA cooperative networks. In [22], a buffer-aided adaptive link scheme for a single-relay NOMA network with an infinite buffer size is proposed, in which the NOMA and OMA transmission can be optimally chosen by letting the buffer operate at the edge of non-absorbing mode. In [23], another buffer-aided NOMA link selection scheme is proposed, where the system model is the same as that in [22] except the buffer size is finite. Because of the limited buffer size, it is usually not possible to have the buffer operating at the non-absorbing edge, making it very hard (if not impossible) to optimally select the link to maximize the throughput. An opportunistic link selection scheme is proposed in [23], in which the relay always applies the NOMA to serve the two users. The proposed scheme however only has higher throughput than its OMA counterpart in the high SNR range. This is because the network throughput can be regarded as $\eta(1 - P_{out})$ in the delay-limited scenario [24], where η is the data rate (without considering the outage) and P_{out} is the outage probability. Compared with the OMA scheme, the NOMA doubles the data rate η but increases the outage probability P_{out}. At the low SNR range, because P_{out} is close to one, the throughput is dominated by P_{out} and the OMA scheme has higher throughput than the NOMA. At the high SNR range, on the other hand, P_{out} approaches zero when the SNR goes to infinity. Then the throughput is determined by η and the NOMA scheme has higher throughput than the OMA. Therefore, when the SNR is not large enough to support NOMA, instead of stop transmitting (as in [23]), the OMA may still be applied. Although authors in [23] suggest switching between the NOMA and OMA based on the outage events, they highlighted (Remark 3, [23]) that combining NOMA and OMA will make the performance analysis "very complicated". A compromise approach is to set a threshold SNR. When the SNR is larger than the threshold, the NOMA buffer-aided scheme is used, and otherwise the OMA scheme is used. As will be shown later in this paper, this compromised approach cannot achieve the full potential of the system.

The performance of buffer-aided cooperative networks depends on buffer states which are determined by the number of packets in buffers. If a relay buffer is full or empty, the corresponding source-to-relay or relay-to-destination link is not available for transmission respectively. The early proposed buffer-aided *max-link* relay selection [25] may achieve full diversity order (i.e. twice the number of relay nodes) when the buffers have infinite size and balanced input/output data rates which is however not always the case in practice. In [26], a buffer state based relay selection scheme is proposed, in which the link selection is based on not only channel gains but also buffer states. The state-based relay selection scheme achieves better outage performance than the max-link scheme, but the improvement becomes less significant for unbalanced channels. This becomes more serious in the NOMA cooperative network:

TABLE I
LIST OF NOTATIONS

K	Relay number	L	Buffer size
h	Channel coefficient	C	Channel capacity
P_t	Transmit power	σ^2	Noise variance
γ	Instantaneous SNR	$\bar{\gamma}$	Average SNR
Ω	Average channel gain	η	Target data rate
P_{out}	Outage probability	α	NOMA power factor
q	Buffer length	$\mathbf{q}$	Buffer state vector
Θ	Target buffer length	Δ	$\lvert q-\Theta\rvert$
$\mathcal{M}$	Priority measurement	$\mathcal{O}(.)$	Selection priority
$\mathbf{A}$	State transition matrix	$\boldsymbol{\pi}$	Steady state vector
ξ	Average throughput	d	Diversity order

even when the source-to-relay and relay-to-destination links have the same average gains, the buffer input/output rate may still be unbalanced because the source-to-relay and relay-to-destination apply different transmission modes. It is interesting to note that the buffer-aided NOMA link selection scheme in [23] uses a similar selection principle as that in [26].

As aforementioned, the optimum link selection in [22] applies to the relay network with infinite buffer sizes which is often impractical. On the other hand, the link selection in [23] considers finite buffer size, but it does not include the OMA transmission and the selection rule is not always optimum. Neither [22] nor [23] considers the multiple relay scenario. This motivates us to investigate the finite size buffer-aided relay selection for cooperative NOMA in the IoT. The main contributions of this paper are listed as following:

- Proposing a novel buffer-aided relay selection scheme for multiple relay cooperative NOMA networks in the IoT.
- Composing a prioritization-based selection rule to seamlessly combine both NOMA and OMA transmission.
- Analyzing the average throughput of the proposed scheme. Combining NOMA and OMA makes the performance analysis very complicated, and considering multiple relays also further complicates the analysis.
- Obtaining the diversity order of the proposed scheme as $3K$, where K is the relay number. In contrast, if the link selection in [23] is generalized to multiple relays, the diversity order would be $2K$.

The rest of the paper is organized as following: Section II describes the system model; Section III proposes the relay selection rule; Section IV analyzes the average network throughput and diversity order; Section V shows simulation results; Finally, Section VI concludes the paper. The list of notations in this paper is given in Table I.

II. SYSTEM MODEL

The system model of the buffer-aided cooperative NOMA in the IoT is shown in Fig. 1, where there are one source node S, K half-duplex decode-and-forward (DF) relay nodes denoted as R_k, $k = 1, \cdots, K$ and two users U_1 and U_2, respectively. The channel coefficients for $S \to R_k$, $R_k \to U_1$ and $R_k \to U_2$ links are denoted as h_{sr_k}, $h_{r_k u_1}$ and $h_{r_k u_2}$ respectively. Every relay R_k is equipped with two L-size buffers for data transmissions to users U_1 and U_2 respectively. We assume that there are no direct links between the source and the two users, and all channels are flat Rayleigh fading that remain constant within the time slot and change independently from one slot to another. Without losing generality, we assume

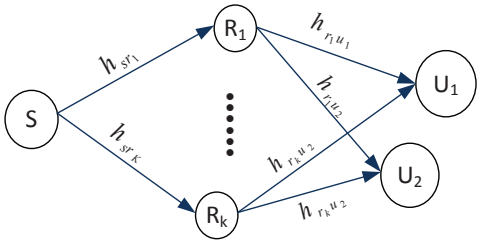

Fig. 1. System model for the cooperative NOMA network in the IoT.

that the transmit powers at all transmit nodes are P_t, and the noise variances at all receiving nodes are σ^2.

When the OMA transmission is applied, at time slot t, the link capacity for channel $h_{d_k}(t)$ is given by

$$C_{d_k}(t) = \log_2(1+\gamma_{d_k}(t)), \quad d_k \in \{sr_k, r_k u_1, r_k u_2\},\ k = 1, \cdots, K, \tag{1}$$

where $\gamma_{d_k}(t) = (P_t/\sigma^2)|h_{d_k}(t)|^2$. Assuming $|h_{d_k}(t)|^2$ is exponentially distributed with the average Ω_{d_k}, $\gamma_{d_k}(t)$ is also exponentially distributed with average $\bar{\gamma}_{d_k} = (P_t/\sigma^2)\Omega_{d_k}$. Thus $\gamma_{d_k}(t)$ and $\bar{\gamma}_{d_k}$ are the instantaneous and average SNR for channel $h_{d_k}(t)$ respectively.

A. Transmission mode

At every time slot, both the $S \to R_k$ and $R_k \to U_m$ transmissions may operate in two modes: double and single packet transmission respectively. For the $S \to R_k$ link, if it satisfies

$$C_{sr_k}(t) \geq 2\eta, \tag{2}$$

where η is the target data rate, the source S is able to transmit two packets to both buffers at R_k. This is achieved based on the TDMA (time-division-multiple-access) principle by applying half of the time slot to transmit each packet. Otherwise, if (2) does not hold but $C_{sr_k}(t) \geq \eta$, a single packet can be transmitted to either of the buffers at R_k. On the other hand, for the $R_k \to U_m$ ($m = 1$ or 2) link, the NOMA can be applied to transmit packets to U_1 and U_2 simultaneously. The superimposed NOMA symbol at R_k is given by

$$x_{r_k}(t) = \sqrt{\alpha}x_{r_{k,1}}(t) + \sqrt{1-\alpha}x_{r_{k,2}}(t), \tag{3}$$

where $x_{r_{k,1}}(t)$ and $x_{r_{k,2}}(t)$ are data for users U_1 and U_2 respectively, and $0 \leq \alpha \leq 1$. Then the received signal at U_m is given by

$$y_m(t) = \sqrt{P_t}h_{r_k u_m}(t)x_{r_k}(t) + n_m(t), \quad m = 1, 2, \tag{4}$$

where $n_m(t)$ is the noise at user U_m. When the NOMA is applied, the link capacity is not given by (1) but must include the interference within the superimposed symbol. To be specific, when $\gamma_{r_k u_1}(t) > \gamma_{r_k u_2}(t)$, the SNR to decode $x_{r_{k,2}}(t)$ at U_2 is given by

$$SNR(x_{r_{k,2}}(t)) = \frac{\sqrt{1-\alpha}\gamma_{r_k u_2}(t)}{\sqrt{\alpha}\gamma_{r_k u_2}(t)+1}, \qquad \text{if } \gamma_{r_k u_1}(t) > \gamma_{r_k u_2}(t). \tag{5}$$

Because $\gamma_{r_k u_1}(t) > \gamma_{r_k u_2}(t)$, $x_{r_{k,2}}(t)$ can also be decoded at U_1 if it can be at U_2. Removing $x_{r_{k,2}}(t)$ from the received signal at U_1, the SNR to decode $x_{r_{k,1}}(t)$ at U_1 is given by

$$SNR(x_{r_{k,1}}(t)) = \sqrt{\alpha}\gamma_{r_k u_1}(t), \qquad \text{if } \gamma_{r_k u_1}(t) > \gamma_{r_k u_2}(t). \tag{6}$$

Following similar procedures as those in [23], the condition that there exists an α to support NOMA transmission to both U_1 and U_2 (i.e. $\log_2(1+SNR(x_{r_{k,m}}(t)) \geq \eta$ for $m=1$ and 2) is given by

$$\gamma_{r_k u_2}(t) \geq \frac{(2^\eta-1)\gamma_{r_k u_1}(t)}{\gamma_{r_k u_1}(t) - 2^\eta(2^\eta-1)}, \quad \text{if } \gamma_{r_k u_1}(t) > \gamma_{r_k u_2}(t). \tag{7}$$

Similarly, if $\gamma_{r_k u_1}(t) < \gamma_{r_k u_2}(t)$, the NOMA condition becomes

$$\gamma_{r_k u_1}(t) \geq \frac{(2^\eta-1)\gamma_{r_k u_2}(t)}{\gamma_{r_k u_2}(t) - 2^\eta(2^\eta-1)}, \quad \text{if } \gamma_{r_k u_1}(t) < \gamma_{r_k u_2}(t). \tag{8}$$

If the SNR for the $R_k \rightarrow U_m$ ($m=1$ or 2) links is not large enough to satisfy (7) or (8), the NOMA transmission is not possible. In this case, if $C_{r_k u_m}(t) > \eta$, the OMA can be used to transmit one packet to U_m.

III. Selection rule

For the relay R_k, the transmission may be chosen from the following six candidates

$$\{(sr_{k,1}),\ (sr_{k,2}),\ (TDMA_k),\ (r_{k,1}u_1),\ (r_{k,2}u_2),\ (NOMA_k)\}, \tag{9}$$

where $(sr_{k,m})$ indicates the single packet transmission from S to the m-th buffer at R_k, $(TDMA_k)$ indicates the double packet transmission based on TDMA from S to both buffers at R_k, $(r_{k,m}u_m)$ is the single transmission from the m-th buffer at R_k to U_m, and $(NOMA_k)$ is the NOMA based double transmission from R_k to both U_1 and U_2. In total, there are $6K$ candidates. The relay selection is to select not only a relay link but also a transmission mode, among all available transmission candidates.

At any time, the numbers of data packets in relay buffers (i.e. the buffer length) form the buffer states. While each relay has two buffers, if the relay number is K and buffer size is L, there are $(L+1)^{2K}$ states in total. The l-th state vector is defined as

$$\mathbf{q}^{(l)} = [q_{1,1}^{(l)}, q_{1,2}^{(l)}, \cdots, q_{K,1}^{(l)}, q_{K,2}^{(l)}], \qquad l = 1, \cdots, (L+1)^{2K}, \tag{10}$$

where $q_{k,m}^{(l)}$ is the buffer length for the m-th buffer at R_k at state $\mathbf{q}^{(l)}$. At any time slot, given the buffer states and channel-state-information (CSI) of all channels, the relay selection is carried out as following:

- First, selection priorities are given to all available transmission candidates. This will be described later.
- All candidates are then checked, from the highest to lowest priorities, whether they can support the target data rate or not. This is meant to check whether (2) is satisfied for candidate $(TDMA_k)$, (7) or (8) for candidate $(NOMA_k)$, and $C_{d_k} > \eta$ for single transmission candidates.
- The candidate with the highest priority which can support the target transmission rate is selected for data transmission.
- Outage occurs if no candidate can be selected.

In order to give priority orders to select the available transmission candidates, we introduce the "target buffer length", $\Theta_{k,m}$, for the m-th buffer ($m=1$ or 2) at relay R_k. Supposing the buffer state is $\mathbf{q}^{(i)}$, the distance between the buffer length and the corresponding target length is defined as

$$\Delta_{k,m}^{(i)} = |q_{k,m}^{(i)} - \Theta_{k,m}|, \qquad m=1,2, \quad k=1,\cdots,K, \tag{11}$$

Then we can give higher priorities to candidates corresponding to buffers further away from the target length as following:

- The double transmission candidates always have higher priority than the single transmission candidates. If an available double transmission candidate $cand_b$ is selected, the buffer lengths of both buffers at relay R_{k_b} are changed by one, and the buffer state becomes $\mathbf{q}^{(i,cand_b)}$. Then for $m=1$ and 2, we obtain

$$\begin{aligned} \Delta_{k_b,m}^{(i,cand_b)} &= |q_{k_b,m}^{(i,cand_b)} - \Theta_{k_b,m}|, \\ cand_b &\in \{(TDMA_{k_b}),\ (NOMA_{k_b})\} \end{aligned} \tag{12}$$

  While selecting $cand_b$ leads to buffer length change of two buffers at relay R_{k_b}, the buffer with higher $\Delta_{k_b,m}^{(i,cand_b)}$ is used for prioritization. Then the priority measurement for selecting candidate $cand_b$ at state $\mathbf{q}^{(i)}$ is defined as

$$\mathcal{M}^{(i,cand_b)} = \text{sign}\left(\Delta_{k_b,m_b}^{(i,cand_b)} - \Delta_{k_b,m_b}^{(i)}\right) \cdot \Delta_{k_b,m_b}^{(i,cand_b)}, \tag{13}$$

  where $m_b = \arg\left\{\max_m \left(\Delta_{k_b,m}^{(i,cand_b)} |\ m=1,2\right)\right\}$. It is clear that, if $\mathcal{M}^{(i,cand_b)} < 0$, selecting $cand_b$ will decrease the distance between the corresponding buffer and target lengths, and otherwise will increase it. Thus higher priority is given to candidates with smaller $\mathcal{M}^{(i,cand_b)}$.
- Similarly, the priorities for single transmission candidates are ordered as follows. If an available single transmission candidate $cand_a$ is selected, the buffer length of the m_a-th buffer at relay R_{k_a} is changed by one so that the buffer state becomes $\mathbf{q}^{(i,cand_a)}$, and then the new distance between the buffer length and the target is given by

$$\begin{aligned} \Delta_{k_a,m_a}^{(i,cand_a)} &= |q_{k_a,m_a}^{(i,cand_a)} - \Theta_{k_a,m_a}|, \\ cand_a &\in \{(sr_{k_a,1}),\ (sr_{k_a,2}),\ (r_{k_a,1}u_1),\ (r_{k_a,2}u_2)\} \end{aligned} \tag{14}$$

  The priority measurement for selecting candidate $cand_a$ is then obtained as

$$\mathcal{M}^{(i,cand_a)} = \text{sign}\left(\Delta_{k_a,m_a}^{(i,cand_a)} - \Delta_{k_a,m_a}^{(i)}\right) \cdot \Delta_{k_a,m_a}^{(i,cand_a)} \tag{15}$$

  Higher priority is then given to candidates with smaller $\mathcal{M}^{(i,cand_a)}$.

The high throughput relies on large data rate and low outage probability. In the proposed scheme, the large data rate is achieved by giving higher priority to select double-packet transmission modes, and the low outage probability is achieved by setting appropriate target lengths so that the buffer lengths are kept away from empty or full as much as possible. In general, for buffers at relay R_k, if the input data rate is higher than the output rate, the buffers are likely to be saturated and thus the target length shall be set close to zero. Otherwise, if the input rate is smaller than the output rate, the buffers tend to be empty and the target buffer length shall be close to the full buffer size. Particularly, if a buffer's input and output rates are the same, the target buffer length can be set as 2 (where we assume the buffer size is larger than 3), because this not only keeps buffer lengths away from empty or full but also leads to small packet delay. In the NOMA scheme, however, the input and output rates at buffers depend on not only channel gains but also transmission modes. Therefore, even if the $S \rightarrow R_k$ and $R_k \rightarrow U_m$ links have the same average SNR, setting the target length to 2 may not be optimum. It is interesting to note that the selection rules in [23], except that it does not include the OMA transmission, is equivalent to the proposed selection rule with the target buffer lengths being set to 2. On the other hand, in order to

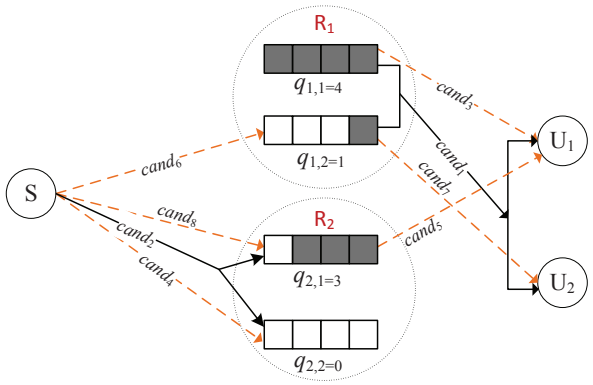

Fig. 2. An example of giving priori orders to available candidates at state $\mathbf{q} = [4, 1, 3, 0]$, where the target buffer length is 2, $cand_m$ indicates the priority order of the corresponding candidate is m, the links with the solid-lines are for the double transmission, and the links with dash-lines are for the single transmission.

achieve minimum transmission delay, the target buffer length shall be set as zero so that the data in the buffers can be transmitted out as quickly as possible[1].

Before leaving this section, we show an example of giving priori orders to all available candidates in Fig. 2, where the relay number $K = 2$, the buffer size $L = 4$, the target buffer lengths for all buffers are set as 2, and the buffer state is $\mathbf{q} = [4, 1, 3, 0]$. From (11), the distance between the buffer length and the target for the four buffers can be obtained as $(2, 1, 1, 2)$ respectively. There are two available double transmission candidates at this state, which are $(TDMA_2)$ and $(NOMA_1)$ respectively. From (13), their priority measurements are obtained as $+2$ and -1 respectively, and then their priorities are given as

$$\mathcal{O}(NOMA_1) > \mathcal{O}(TDMA_2), \tag{16}$$

where $\mathcal{O}(.)$ is the selection priority for the enclosed candidate. On the other hand, there are six single transmission candidates, which are $(sr_{1,2})$, $(r_{1,1}u_1)$, $(r_{1,2}u_2)$, $(sr_{2,1})$, $(sr_{2,2})$ and $(r_{2,1}u_1)$ respectively. From (15), the priority measurements are obtained as $(0,\ -1,\ +2,\ +2,\ -1,\ 0)$ respectively. Thus the six candidates are prioritized as $\mathcal{O}(r_{1,1}u_1) > \mathcal{O}(sr_{2,2}) > \mathcal{O}(r_{2,1}u_1) > \mathcal{O}(sr_{1,2}) > \mathcal{O}(r_{1,2}u_2) > \mathcal{O}(sr_{2,1})$. The priorities for all available candidates are illustrated in Fig. 2, where $cand_m$ indicates the priority order of the corresponding candidate is m.

IV. Average Throughput

Let $\mathbf{A}$ be the $(L+1)^{2K} \times (L+1)^{2K}$ state transition matrix, where the entry $A_{i,j}$ as the transition probability from state $\mathbf{q}^{(j)}$ to $\mathbf{q}^{(i)}$. Particularly $A_{i,i}$ is the outage probability at state $\mathbf{q}^{(i)}$. We assume that at buffer state $\mathbf{q}^{(i)}$, there are L_i available candidates for selection at state $\mathbf{q}^{(i)}$, denoted as $cand_1, \cdots, cand_{L_i}$ from the highest to the lowest priority order respectively.

Every double transmission candidate is associated with a pair of single transmission candidates: candidate $(TDMA_k)$ is associated with $(sr_{k,1})$ and $(sr_{k,2})$, and candidate $(NOMA_k)$ is associate with $(r_{k,1}u_1)$ and $(r_{k,2}u_2)$. We have the following remarks:

Remark 1: A double transmission candidate and its two associated single transmissions are not independent, because they correspond to the same link(s).

[1]This paper focuses on the network throughput. The details for the network delay is being studied in our another work.

Remark 2: If a single transmission candidate is in outage, its associated double transmission candidate must also be in outage.

Below we derive the transition probability $A_{i,j}$ for $i = j$ and $i \neq j$, from which the average throughput is obtained. For better exposition, we will show the analysis for the example in Fig. 2. As is shown in Fig. 2, there are eight available candidates for selection at state $\mathbf{q}^{(i)} = [4, 1, 3, 0]$, in which candidates $\{cand_1, cand_3, cand_7\}$ are associated, so are the candidates $\{cand_2, cand_4, cand_8\}$, but $cand_l$ and $cand_l$ are not associated with any other candidates. We denote $P(\overline{cand_l})$ and $P(cand_l)$ as the probabilities that the candidate $cand_l$ is and not in outage, respectively.

A. The outage probability at state $\mathbf{q}^{(i)}$: $A_{i,i}$

The outage probability at state $\mathbf{q}^{(i)}$ is the probability that all available candidates are in outage as

$$P_{out}^{\mathbf{q}^{(i)}} = A_{i,i} = P(\overline{cand}_1, \cdots, \overline{cand}_{L_i}). \tag{17}$$

For the example in Fig. 2, from remark 1, we have

$$\begin{aligned} P_{out}^{\mathbf{q}^{(i)}=[4,1,3,0]} &= P((\overline{NOMA_1}), \overline{cand}_3, \overline{cand}_7) \\ &\times P(\overline{TDMA_2}, \overline{cand}_4, \overline{cand}_8) P(\overline{cand}_5) P(\overline{cand}_6), \end{aligned} \tag{18}$$

where candidates $cand_1$ and $cand_2$ are represented as $(NOMA_1)$ and $(TDMA_2)$ respectively for better exposition. From remark 2, we have

$$\begin{aligned} P((\overline{NOMA_1}), \overline{cand}_3, \overline{cand}_7) &= P(\overline{cand}_3, \overline{cand}_7) \\ &= P(\overline{cand}_3) P(\overline{cand}_7), \end{aligned} \tag{19}$$

where the second equation comes from the fact that, if candidate $(\overline{NOMA_1})$ is removed, $cand_3$ and $cand_4$ become independent as they correspond to two independent channels. We also have

$$P(\overline{TDMA_2}, \overline{cand}_4, \overline{cand}_8) = P(\overline{cand}_4, \overline{cand}_8) = P(\overline{cand}_4), \tag{20}$$

where the second equation follows from the fact that both $cand_4$ and $cand_8$ correspond to channel h_{sr_2}, leading to duplicate $S \to R_k$ terms in (20).

Substituting (19) and (20) into (18) gives

$$P_{out}^{\mathbf{q}^{(i)}=[4,1,3,0]} = P(\overline{cand}_3) P(\overline{cand}_7) P(\overline{cand}_4) P(\overline{cand}_5) P(\overline{cand}_6). \tag{21}$$

Every term in (21) corresponds to one single packet transmission. This can be straightforwardly extended to general cases: i.e. the outage probability at state $\mathbf{q}^{(i)}$ can be obtained by removing all double-transmission and duplicate $S \to R_k$ link terms in (17). Candidates $(sr_{k,m})$ and $(r_k u_m)$ correspond to channels h_{sr_k} and $h_{r_k u_m}$ respectively. Supposing $cand_w$ corresponds to channel h_{d_k}, from (1), we have

$$\begin{aligned} P(\overline{cand}_w) = P\{\log_2(1 + \gamma_{d_k}(t)) < \eta\} = 1 - e^{\left(-\frac{2^\eta - 1}{\bar{\gamma}_{d_k}}\right)}, \\ d_k \in \{sr_k, r_{k,1}u_1, r_{k,2}u_2\}. \end{aligned} \tag{22}$$

For the example in Fig. 2, $cand_3, \cdots, cand_7$ correspond to channels $h_{r_1 u_{1,1}}$, h_{sr_2}, $h_{r_2 u_{2,1}}$, h_{sr_1} and $h_{r_1 u_{1,2}}$ respectively.

The above analysis leads to the following remark:

Remark 3: The outage probability at any state depends only on the available single packet transmission candidates

B. The transition probability at state $\mathbf{q}^{(i)}$: $A_{j,i}$

We suppose that if $cand_l$ is selected, the buffer state transits from $\mathbf{q}^{(i)}$ to $\mathbf{q}^{(i_l)}$, which occurs when all candidates with higher

priority order than $cand_l$ are in outage and $cand_l$ is not in outage. Thus we have

$$A_{i_l,i} = P(\overline{cand}_1, \cdots, \overline{cand}_{l-1}, cand_l). \tag{23}$$

1) $cand_l$ is a double transmission candidate: Because double transmission candidates have higher priority than the single transmission candidates, no single transmission term is included in (23). In the example shown in Fig. 2, we have

$$\begin{aligned} A_{i_1,i} =& P(cand_1) = P((NOMA_1)) = 1 - P((\overline{NOMA_1})) \\ A_{i_2,i} =& P(\overline{cand}_1, cand_2) = P(\overline{cand}_1)P(cand_2) \\ =& P((\overline{NOMA_1}))(1 - P((\overline{TDMA_2})), \end{aligned} \tag{24}$$

where

$$P((\overline{NOMA_k})) = 1 - P_{k,(1,2)} - P_{k,(2,1)}, \tag{25}$$

where $P_{k,(1,2)}$ and $P_{k,(2,1)}$ are the probabilities that the NOMA can be supported for (7) and (8) respectively. Following the similar procedures as those in [23], we have

$$\begin{aligned} P_{k,(m,n)} =& \frac{1}{\bar{\gamma}_{r_k u_m}} e^{\left(-\frac{(2^{\eta}-1)\bar{\gamma}_{r_k u_m} + (2^{2\eta}-2^{\eta})\bar{\gamma}_{r_k u_n}}{\bar{\gamma}_{r_k u_m}\bar{\gamma}_{r_k u_n}}\right)} \\ & \times \int_{2^{\eta}-1}^{\infty} e^{\left(-\frac{x}{\bar{\gamma}_{r_k u_m}} - \frac{2^{\eta}(2^{\eta}-1)^2}{\bar{\gamma}_{r_k u_n} x}\right)} \mathrm{d}x \\ & - \frac{\bar{\gamma}_{r_k u_n}}{\bar{\gamma}_{r_k u_m} + \bar{\gamma}_{r_k u_n}} e^{\left(-\frac{(2^{\eta}-1)(\bar{\gamma}_{r_k u_m} + \bar{\gamma}_{r_k u_n})(2^{2\eta}+2^{\eta})}{\bar{\gamma}_{r_k u_m}\bar{\gamma}_{r_k u_n}}\right)}, \end{aligned} \tag{26}$$

where $(m,n) \in \{(1,2),(2,1)\}$. On the other hand, we have

$$P((\overline{TDMA_k})) = P\{\log_2(1+\gamma_{sr_k}(t)) < 2\eta\} = 1 - e^{\left(-\frac{2^{2\eta}-1}{\bar{\gamma}_{sr_k}}\right)}. \tag{27}$$

2) $cand_l$ is a single transmission candidate: For the example in Fig. 2, the transition probabilities when candidates $cand_3, \cdots, cand_6$ are selected are respectively obtained as

$$\begin{aligned} A_{i_3,i} &= P(\overline{(NOMA_1)}, cand_3)P(\overline{(TDMA_2)}) \\ A_{i_4,i} &= P(\overline{(NOMA_1)}, \overline{cand}_3)P(\overline{(TDMA_2)}, cand_4) \\ &= P(\overline{cand}_3)P(\overline{(TDMA_2)}, cand_4) \\ A_{i_5,i} &= P(\overline{(NOMA_1)}, \overline{cand}_3)P(\overline{(TDMA_2)}, \overline{cand}_4)P(cand_5) \\ &= P(\overline{cand}_3)P(\overline{cand}_4)P(cand_5) \\ A_{i_6,i} &= P(\overline{(NOMA_1)}, \overline{cand}_3)P(\overline{(TDMA_2)}, \overline{cand}_4)P(\overline{cand}_5) \\ &\quad \times P(cand_6) \\ &= P(\overline{cand}_3)P(\overline{cand}_4)P(\overline{cand}_5)P(cand_6). \end{aligned} \tag{28}$$

On the other hand, we obtain the transition probabilities when candidates $cand_7$ and $cand_8$ are selected as

$$\begin{aligned} A_{i_7,i} &= P(\overline{(NOMA_1)}, \overline{cand}_3, cand_7)P(\overline{(TDMA_2)}, \overline{cand}_4) \\ &\quad \times P(\overline{cand}_5)P(\overline{cand}_6) \\ &= P(\overline{cand}_3, cand_7)P(\overline{cand}_4)P(\overline{cand}_5)P(\overline{cand}_6) \\ &= P(\overline{cand}_3)P(cand_7)P(\overline{cand}_4)P(\overline{cand}_5)P(\overline{cand}_6) \\ A_{i_8,i} &= P(\overline{(NOMA_1)}, \overline{cand}_3, \overline{cand}_7)P(\overline{cand}_5)P(\overline{cand}_6) \\ &\quad \times P(\overline{(TDMA_2)}, \overline{cand}_4, cand_8) \\ &= P(\overline{cand}_3, \overline{cand}_7)P(\overline{cand}_4, cand_8)P(\overline{cand}_5)P(\overline{cand}_6) \\ &= 0, \end{aligned} \tag{29}$$

where we make use of $P(\overline{cand}_3, cand_7) = P(\overline{cand}_3)P(cand_7)$ and $P(\overline{cand}_4, cand_8) = 0$ in obtaining (29).

Furthermore, we have

$$\begin{aligned} P((\overline{NOMA_k}), (r_{k,m}u_m)) &= 1 - P((\overline{NOMA_k}), \overline{(r_{k,m}u_m)}) \\ &\quad - P((NOMA_k), (r_{k,m}u_m)) - P((NOMA_k), \overline{(r_{k,m}u_m)}). \end{aligned} \tag{30}$$

From remark 2, we have $P((\overline{NOMA_k}), \overline{(r_{k,m}u_m)}) = P(\overline{(r_{k,m}u_m)})$, $P((NOMA_k), (r_{k,m}u_m)) = P((NOMA_k))$ and $P((NOMA_k), \overline{(r_{k,m}u_m)}) = 0$. Substituting these into (30) gives

$$\begin{aligned} P((\overline{NOMA_k}), (r_{k,m}u_m)) &= 1 - P(\overline{(r_{k,m}u_m)}) - P((NOMA_k)) \\ &= P((\overline{NOMA_k})) - P(\overline{(r_{k,m}u_m)}), \end{aligned} \tag{31}$$

where $P((\overline{NOMA_k}))$ and $P(\overline{(r_{k,m}u_m)})$ are obtained in (25) and (22) respectively. Similarly we have

$$\begin{aligned} & P((\overline{TDMA_k}), (sr_{k,m})) \\ &= 1 - P((\overline{TDMA_k}), \overline{(sr_{k,m})}) - P((TDMA_k), (sr_{k,m})) \\ &\quad - P((TDMA_k), \overline{(sr_{k,m})}) \\ &= 1 - P(\overline{(sr_{k,m})}) - P((TDMA_k)) \\ &= P((\overline{TDMA_k})) - P(\overline{(sr_{k,m})}), \end{aligned} \tag{32}$$

where $P((\overline{TDMA_k}))$ and $P(\overline{(sr_{k,m})})$ are obtained in (27) and (22) respectively. It is straightforward to extend the above analysis to general cases that the transition probability $A_{j,i}$ can always be decomposed into terms including $P((\overline{NOMA_k}))$, $P((\overline{TDMA_k}))$ and $P(\overline{cand}_w)$, where $cand_w$ is a single transmission candidate.

The above analysis leads to the following remark:

Remark 4: The double packet transmission candidates have higher priority to determine the transmission probabilities than the single packet transmission. Only when the double transmission candidates are not available or in outage, do the single transmissions affect the transition probabilities.

C. Throughput

From (17) and (23), we can obtain the transition matrix $\mathbf{A}$. Because $\mathbf{A}$ is irreducible and aperiodic[2], the steady state distribution of the Markov chain is given by

$$\boldsymbol{\pi} = (\mathbf{A} - \mathbf{I} + \mathbf{B})^{-1}\mathbf{b}, \tag{33}$$

where $\boldsymbol{\pi} = [\pi_1, \pi_2, \cdots, \pi_{(L+1)^{2K}}]$, π_l is the probability that the buffer state is $\mathbf{q}_l$, $\mathbf{b} = [1, \cdots, 1]^T$, $\mathbf{I}$ denotes the identity matrix and $\mathbf{B}$ denotes an $(L+1)^{2K} \times (L+1)^{2K}$ matrix with all elements of one.

At any time slot, if candidate $(r_{k,1}u_1)$ or $(r_{k,2}u_2)$ is selected, one packet is transmitted to user U_1 or U_2, respectively. While if candidate $(NOMA_k)$ is selected, two packets are transmitted from R_k to the users. At state $\mathbf{q}^{(i)}$, the probabilities to select candidates $(r_{k,1}u_1)$, $(r_{k,2}u_2)$ and $(NOMA_k)$ are denoted as $P^{(i)}_{r_{k,1}u_1}$, $P^{(i)}_{r_{k,2}u_2}$ and $P^{(i)}_{NOMA_k}$ respectively, which are zero if the corresponding candidates are not available at state $\mathbf{q}^{(i)}$ and otherwise are obtained

[2]The Markov chain is irreducible if all states are reachable starting from any state. If the probability of staying at any state higher than zero, the Markov chain is aperiodic [27]

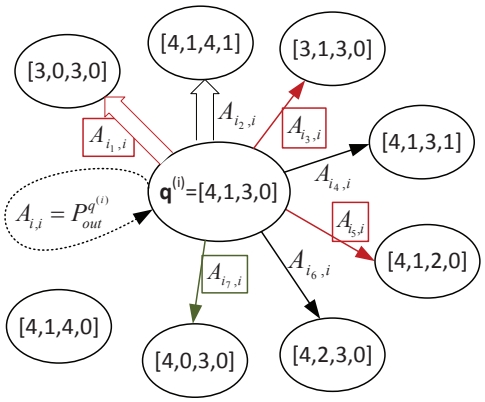

Fig. 3. State transition diagram at the state $\mathbf{q}^{(i)} = [4,1,3,0]$ for the example in Fig. 2, where the single and double arrows represent the state transitions due to the single and double packet transmissions respectively.

as in (23). Considering all buffer states and all relay nodes, the average throughput for user U_m is given by

$$\xi_m = \sum_{i=1}^{(L+1)^2} \pi_i \xi_m^{(i)} = \sum_{i=1}^{(L+1)^2} \pi_i \sum_{k=1}^{K} \left(P_{r_k u_m}^{(i)} + P_{NOMA_k}^{(i)} \right), \quad (34)$$

where $m \in \{1,2\}$, $\xi_m^{(i)} = \sum_{k=1}^{K} \left(P_{r_k u_m}^{(i)} + P_{NOMA_k}^{(i)} \right)$ which is the average throughput for user U_m at state $\mathbf{q}^{(i)}$. And the overall throughput for all users is given by $\xi = \xi_1 + \xi_2$.

For illustration, Fig. 3 shows all possible buffer state transition at the state $\mathbf{q}^{(i} = [4,1,3,0]$ for the example in Fig. 2, where the single and double arrows represent the state transitions due to the single and double packet transmission, respectively. The average throughputs for users U_1 and U_2 at this state are given by $\xi_1^{(i)} = A_{i_1,i} + A_{i_3,i} + A_{i_5,i}$ and $\xi_2^{(i)} = A_{i_1,i} + A_{i_7,i}$ respectively.

D. Diversity order

The diversity order is defined as

$$d = -\lim_{\bar{\gamma}\to\infty} \frac{\log P_{out}}{\log \bar{\gamma}}, \quad (35)$$

where $\bar{\gamma} = P_t/\sigma^2$ and P_{out} is the outage probability of the system which is given by

$$P_{out} = \sum_i P_{out}^{\mathbf{q}^{(i)}} \pi_i. \quad (36)$$

The diversity order depends on both the outage probabilities at every state $P_{out}^{\mathbf{q}^{(i)}}$ and the stationary buffer state probabilities π_i.

When $\bar{\gamma} \to \infty$, all transmission candidates are able to support the target rate transmission. Thus if the target buffer length is set as $2 \le \Theta_i < L$ (where we assume the buffer size $L \ge 3$), according to the proposed prioritization-based selection rule, the buffer lengths at any time slot are either Θ_i or $\Theta_i - 1$ which are neither empty nor full. From Remark 4, the transition probabilities are then only determined by the double transmission candidates (because they are all available), and the buffers can only be in two states: either all buffer lengthes are Θ_i, or only the pair of buffers for one of the relays have length of $\Theta_i - 1$ and all other buffer lengthes are Θ_i. In both cases, the corresponding $P_{out}^{\mathbf{q}^{(i)}}$ are the same. Further from Remark 3, $P_{out}^{\mathbf{q}^{(i)}}$ only depends on the single transmission candidates which are also all available. Therefore, if the target buffer length is set as $2 \le \Theta_i < L$, we have

$$\begin{aligned} d &= -\lim_{\bar{\gamma}\to\infty} \frac{\log P_{out}}{\log \bar{\gamma}} = -\lim_{\bar{\gamma}\to\infty} \frac{\log P_{out}^{\mathbf{q}^{(i)}}}{\log \bar{\gamma}} \\ &= -\lim_{\bar{\gamma}\to\infty} \frac{\log \prod_{m=k}^{K} P(C_{sr_k} < \eta) P(C_{r_k u_1} < \eta) P(C_{r_k u_2} < \eta)}{\log \bar{\gamma}} \\ &= 3K, \end{aligned} \quad (37)$$

where (22) is substituted in the second equation of above to give the final result. This states that every relay contributes 3 diversity orders to the system, corresponding to $S \to R_k$, $R_k \to U_1$ and $R_k \to U_2$ transmission respectively. It is interesting to note that if only the NOMA transmission is applied (as in [23]), the diversity order is $2K$.

E. Discussion

Below we explain that the proposed scheme has higher sum throughput than both buffer-aided NOMA and OMA schemes. Recall that the network throughput can be regarded as $\eta(1-P_{out})$, where η is the data rate (without considering the outage). From Remark 3, the outage probability of the proposed scheme depends on the single packet transmission, which is significantly lower than that of the buffer-aided NOMA relay selection (which only applies the double packet transmission). On the other hand, because the proposed scheme gives higher priority to the double packet transmission than the single packet transmission, the double packet transmission will always be selected first when possible. This implies that the data rate η of the proposed scheme is no less than that of the NOMA scheme. Thus we have

$$\xi_{proposed} > \xi_{NOMA}, \quad (38)$$

where $\xi_{proposed}$ and ξ_{NOMA} are the sum throughput for the proposed and buffer-aided NOMA schemes respectively. On the other hand, compared with the buffer-aided OMA scheme (which only applies single packet transmission), the proposed scheme has similar outage probability but higher data rate. Thus we also have

$$\xi_{proposed} > \xi_{OMA}, \quad (39)$$

where ξ_{OMA} is the sum throughput for the OMA scheme.

As is mentioned in the introduction section, a simple alternative to combine the NOMA and OMA in the buffer-aided relay selection is to set an appropriate threshold SNR, SNR_t, where $\xi_{NOMA} < \xi_{OMA}$ for $SNR \le SNR_t$, and $\xi_{NOMA} > \xi_{OMA}$ for $SNR > SNR_t$. Then we can simply apply the buffer-aided OMA scheme if $SNR < SNR_t$ and switch to the NOMA scheme otherwise. It is clear the throughput of the switch-based scheme satisfies

$$\xi_{switch} = \begin{cases} \xi_{OMA}, & \text{if } SNR \le SNR_t, \\ \xi_{NOMA}, & \text{if } SNR > SNR_t. \end{cases} \quad (40)$$

Using (38) and (39) in (40), it is clear that the proposed scheme has higher throughput than the switch-based scheme as

$$\xi_{proposed} > \xi_{switch}. \quad (41)$$

V. Numerical Simulations

In all simulations below, the target transmission rate for both users is set to $\eta_1 = \eta_2 = 2$ bps/Hz, the buffer size is set to $L = 5$ for every buffer and all noise powers σ^2 are normalized to unity.

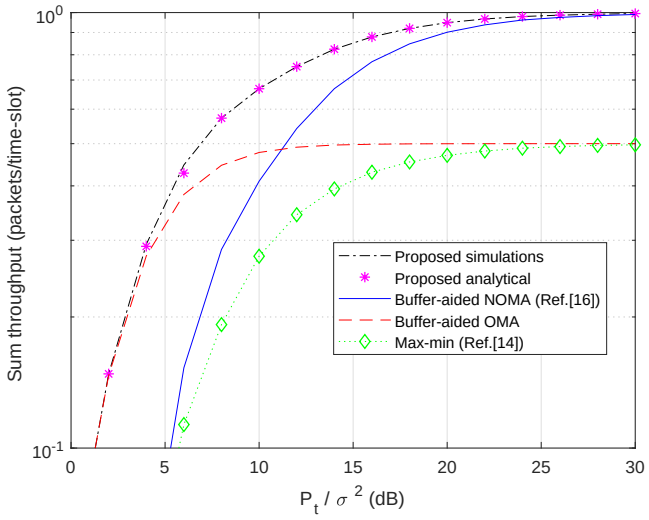

Fig. 4. Throughput of the buffer-aided NOMA, OMA and proposed schemes, where the relay number $K = 1$, buffer size $L = 5$.

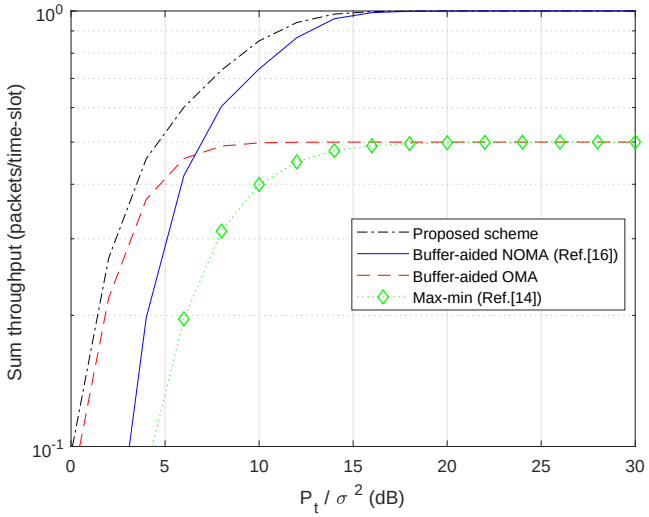

Fig. 5. Throughput of the max-min, buffer-aided NOMA, OMA and proposed schemes, where the relay number $K = 2$ and buffer size $L = 5$.

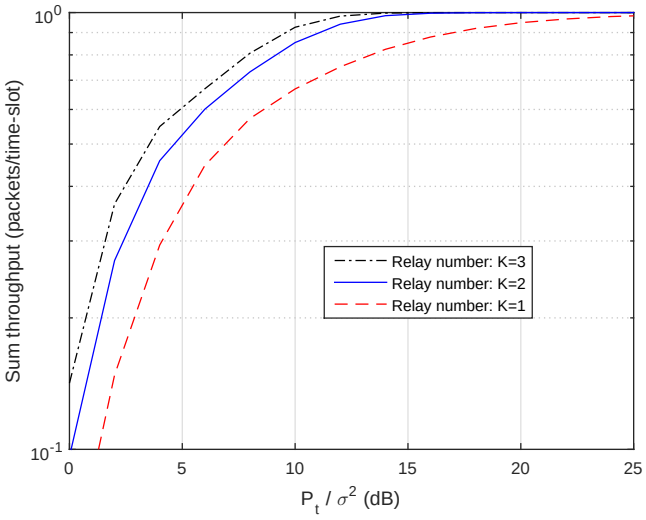

(a) Sum throughput

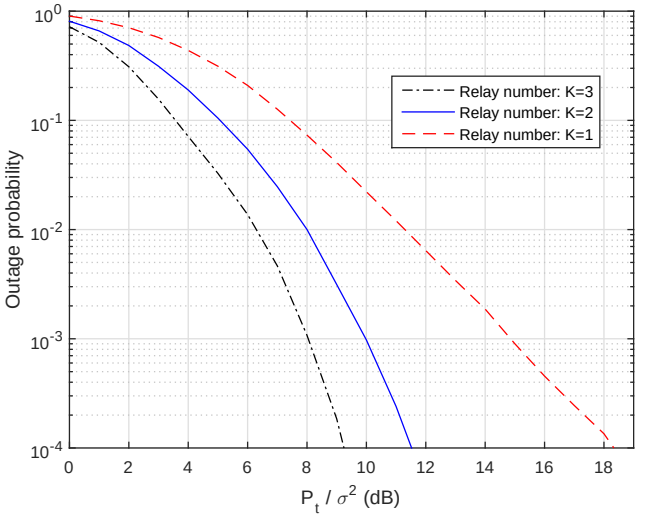

(b) Outage probability

Fig. 6. Throughput and outage probability of the proposed scheme for different relay numbers, where all average channel gains are set to 1 dB and the target buffer length is set to 3.

First we consider the single relay scenario. This is for easy comparison with the buffer-aided NOMA scheme in [23] which considers the same scenario. The average channel gains are set to $\Omega_{sr_1} = 1.1$ dB, $\Omega_{r_1u_1} = 1.0$ dB and $\Omega_{r_1u_2} = 1.5$ dB. Fig. 4 shows the sum throughput *vs* P_t/σ^2 for the proposed scheme, the buffer-aided NOMA scheme in [23], the buffer-aided OMA scheme and the traditional non-buffer-aided max-min scheme. The buffer-aided OMA scheme uses the same selection rule as that in the proposed scheme except the NOMA transmissions are not included in the selection process. The target buffer-lengths in both the proposed and OMA schemes are set to 3.

It is clearly shown in Fig. 4 that the analytical results very well match the simulation results for the proposed scheme, which verifies the analysis in Section IV. Fig. 4 also shows that both buffer-aided NOMA and the proposed scheme can achieve full throughput rate, i.e. one packet/time-slot, when the SNR is large enough. On the other hand, the OMA scheme can only achieve the maximum throughput of 1/2 packet/time-slot. This is because the NOMA delivers two packets simultaneously. As is expected, the NOMA scheme has larger throughput than the OMA over the high SNR range (i.e. $P_t/\sigma^2 > 12$ dB), but has worse throughput than the latter over the low SNR range (i.e. $P_t/\sigma^2 < 12$ dB). On the contrary, the proposed scheme can achieve significant throughput improvement over both low and high SNR ranges. It is interesting to observe that, if we simply apply the switch-based scheme in which the buffer-aided OMA scheme is used in the low SNR range (i.e. $P_t/\sigma^2 < 12$ dB) and the buffer-aided NOMA scheme is used in the high SNR range (i.e. $P_t/\sigma^2 > 12$ dB), the throughput will still be significantly lower than that in the proposed scheme. This well verifies (41) in the discussions in Section IV. In all cases, the non-buffer-aided max-min scheme has the lowest throughput.

Fig. 5 shows the sum throughput for the 2-relay network, where the average channel gains are set to $\Omega_{sr_1} = \Omega_{sr_2} = 1.1$ dB, $\Omega_{r_1u_1} = \Omega_{r_2u_1} = 1$ dB and $\Omega_{r_1u_2} = \Omega_{r_2u_2} = 1.5$ dB. We note that the result for the "buffer-aided NOMA" scheme is based on the generalization of the scheme in [23] (which only considers

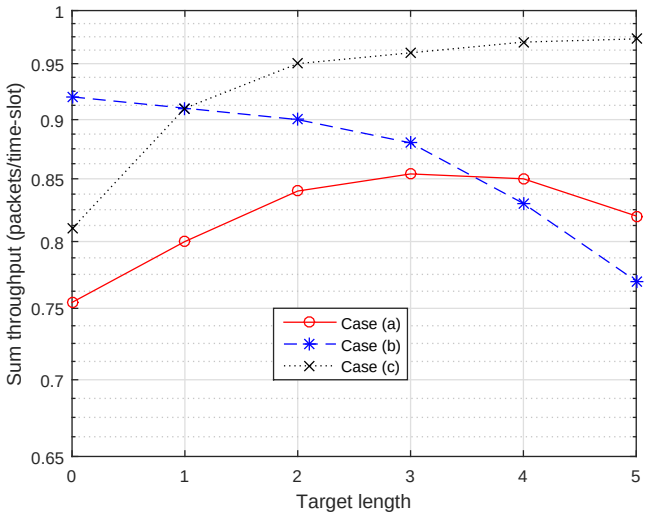

Fig. 7. Throughput *vs* target buffer lengths for the 2-relay network. Case (a): $\bar{\gamma}_{sr_1} = \bar{\gamma}_{sr_2} = \bar{\gamma}_{r_1u_1} = \bar{\gamma}_{r_1u_2} = \bar{\gamma}_{r_2u_1} = \bar{\gamma}_{r_2u_2} = 7$ dB; Case (b): $\bar{\gamma}_{sr_1} = \bar{\gamma}_{sr_2} = 10\bar{\gamma}_{r_1u_1} = 10\bar{\gamma}_{r_1u_2} = 10\bar{\gamma}_{r_2u_1} = 10\bar{\gamma}_{r_2u_2} = 10$ dB; Case (c): $\bar{\gamma}_{r_1u_1} = \bar{\gamma}_{r_1u_2} = \bar{\gamma}_{r_2u_1} = \bar{\gamma}_{r_2u_2} = 30\bar{\gamma}_{sr_1} = 30\bar{\gamma}_{sr_2} = 13$ dB.

TABLE II
DIVERSITY ORDERS

K	$P_{out}(P_t/\sigma^2)$ (dB)	$P_{out}(P_t/\sigma^2)$ (dB)	Diversity order
1	$P_{out}(18 \text{ dB}) = 38.7$	$P_{out}(20 \text{ dB}) = 44.6$	$\frac{44.6-38.7}{20-18} \simeq 3$
2	$P_{out}(10 \text{ dB}) = 30.1$	$P_{out}(11 \text{ dB}) = 36.2$	$\frac{36.2-30.1}{11-10} \simeq 6$
3	$P_{out}(8 \text{ dB}) = 29.6$	$P_{out}(9 \text{ dB}) = 38.5$	$\frac{38.5-29.6}{9-8} \simeq 9$

single relay) by excluding the OMA transmission modes from the proposed scheme. It is clearly shown in Fig. 5 that, while all of the three schemes achieve higher throughput than those in Fig. 4, the comparison among the three schemes is similar.

Fig. 6 (a) and (b) show the throughput and outage probability of the proposed scheme for different relay numbers respectively, where the target buffer length is set to 3 in all cases. Fig. 6 (a) shows that higher throughput is achieved with more relay nodes. This is because of the higher diversity order with more relays as in shown in Fig. 6 (b). According to (35), the diversity orders are calculated in Table II. It is clearly shown that the diversity order is approximately $3K$ which well matches the analysis in (37).

Fig. 7 shows the sum throughput *vs* the target buffer lengths for the proposed scheme for the 2-relay network. Three cases are considered. In case (a), all channels have the same average gains ($\bar{\gamma}_{sr_1} = \bar{\gamma}_{sr_2} = \bar{\gamma}_{r_1u_1} = \bar{\gamma}_{r_1u_2} = \bar{\gamma}_{r_2u_1} = \bar{\gamma}_{r_2u_2} = 7$ dB). As is mentioned earlier, the selection rule in [23] is equivalent to that in the proposed scheme (except the NOMA and OMA combination) by setting the target buffer length to $\Theta_k = 2$. Because $S \to R_k$ and $R_k \to U_m$ apply different transmission modes, even with the same average gains for all channels, the input/output rate at the buffers is still not balanced so that the optimum target length is not two. This is clearly shown in Case (a) where the optimum target length which achieves the largest throughput is three. In Case (b), $S \to R_k$ channels are much stronger than the $R_k \to U_m$ channels where $\bar{\gamma}_{sr_1} = \bar{\gamma}_{sr_2} = 10\bar{\gamma}_{r_1u_1} = 10\bar{\gamma}_{r_1u_2} = 10\bar{\gamma}_{r_2u_1} = 10\bar{\gamma}_{r_2u_2} = 10$ dB, so that the buffers are likely to be saturated. As a result, the optimum target length shall be close to zero, which is clearly verified in Case (b). In Case (c), on the other hand, the $S \to R_k$ channels have much lower average gains than the $R_k \to U_m$ channels where we set as $\bar{\gamma}_{r_1u_1} = \bar{\gamma}_{r_1u_2} = \bar{\gamma}_{r_2u_1} = \bar{\gamma}_{r_2u_2} = 30\bar{\gamma}_{sr_1} = 30\bar{\gamma}_{sr_2} = 13$ dB, and so the buffers tend to be empty. In this case, the optimum target length shall be chosen close to the full buffer size. These results very well match the statements in Section III.

VI. CONCLUSIONS

This paper proposes a buffer-aided relay selection scheme to seamlessly include both NOMA and OMA transmission in the IoT. The proposed scheme achieves significant improvements in throughput over both low and high SNR ranges. A prioritization-based selection rule is described by introducing the target buffer length for every relay buffer. The analytical expression of the average throughput is successfully obtained and verified by numerical simulations. Particularly the diversity order of the proposed scheme is obtained as $3K$, where K is the relay number. This provides useful insight for designing the cooperative NOMA for IoT applications.

REFERENCES

[1] G. Chen, J. Tang, and J. P. Coon, "Optimal routing for multihop social-based d2d communications in the internet of things," *IEEE Internet of Things Journal*, vol. 5, no. 3, pp. 1880–1889, June, 2018.

[2] G. Chen, J. P. Coon, A. Mondal, B. Allen, and J. A. Chambers, "Performance analysis for multi-hop full-duplex iot networks subject to poisson distributed interferers," *IEEE Internet of Things Journal*, pp. 1–1, 2018.

[3] G. Gui, H. Huang, Y. Song, and H. Sari, "Deep learning for an effective non-orthogonal multiple access scheme," *IEEE Trans. Veh. Technol*, vol. 67, pp. 8440–8450, Sep. 2018.

[4] Z. Ding, F. Adachi, and H. V. Poor, "The application of mimo to non-orthogonal multiple access," *IEEE Trans. Wireless Commun.*, vol. 15, pp. 537–552, Jan 2016.

[5] Z. Ding, R. Schober, and H. V. Poor, "A general mimo framework for noma downlink and uplink transmission based on signal alignment," *IEEE Trans. Wireless Commun.*, vol. 15, pp. 4438–4454, Jun 2016.

[6] H. Huang, J. Xiong, J. Yang, G. Gui, and H. Sari, "Jrate region analysis in a full-duplex-aided cooperative nonorthogonal multiple-access system," *IEEE Access*, vol. 5, pp. 17869–17880, Aug. 2017.

[7] K. Lai, J. Lei, L. Wen, G. Chen, W. Li, and P. Xiao, "Secure transmission with randomized constellation rotation for downlink sparse code multiple access system," *IEEE Access*, vol. 6, pp. 5049–5063, 2018.

[8] T. Lv, Y. Ma, J. Zeng, and P. T. Mathiopoulos, "Millimeter-wave NOMA transmission in cellular M2M communications for internet of things," *IEEE Internet of Things Journal*, vol. 5, no. 3, pp. 1989–2000, June, 2018.

[9] M. Liu, T. Song, and G. Gui, "Deep cognitive perspective: Resource allocation for NOMA based heterogeneous IoT with imperfect SIC," *IEEE Internet of Things Journal*, pp. 1–1, 2018.

[10] L. P. Qian, A. Feng, Y. Huang, Y. Wu, B. Ji, and Z. Shi, "Optimal SIC ordering and computation resource allocation in MEC-aware NOMA NB-IoT networks," *IEEE Internet of Things Journal*, pp. 1–1, 2018.

[11] Z. Ding, H. Dai, and H. V. Poor, "Relay selection for cooperative NOMA," *IEEE Wire. Communi. Lett.*, vol. 5, pp. 416–419, Aug 2016.

[12] D. Deng, L. Fan, X. Lei, W. Tan, and D. Xie, "Joint user and relay selection for cooperative NOMA networks," *IEEE Access*, vol. 5, pp. 20220–20227, Sep. 2017.

[13] J. Zhao, Z. Ding, P. Fan, Z. Yang, and G. K. Karagiannidis, "Dual relay selection for cooperative NOMA with distributed space time coding," *IEEE Access*, vol. 6, pp. 20440–20450, April 2018.

[14] N. Nomikos, T. Charalambous, I. Krikidis, D. N. Skoutas, D. Vouyioukas, M. Johansson, and C. Skianis, "A survey on buffer-aided relay selection," *IEEE Communications Surveys Tutorials*, vol. 18, pp. 1073–1097, Secondquarter 2016.

[15] Z. Tian, G. Chen, Y. Gong, Z. Chen, and J. A. Chambers, "Buffer-aided max-link relay selection in amplify-and-forward cooperative networks," *IEEE Transactions on Vehicular Technology*, vol. 64, no. 2, pp. 553–565, Feb. 2015.

[16] Z. Tian, Y. Gong, G. Chen, Z. Chen, and J. Chambers, "Buffer-aided link selection with network coding in multihop networks," *IEEE Trans. Veh. Tech.*, vol. 65, no. 9, pp. 7195–7206, Sep. 2016.

[17] Z. Tian, Y. Gong, G. Chen, and J. A. Chambers, "Buffer-aided relay selection with reduced packet delay in cooperative networks," *IEEE Trans. Veh. Tech.*, vol. 66, no. 3, pp. 2567–2575, Mar. 2017.

[18] A. Bletsas, A. Khisti, D. P. Reed, and A. Lippman, "A simple cooperative diversity method based on network path selection," *IEEE J. Sel. Areas Commun.*, vol. 24, no. 3, pp. 659–672, Mar. 2006.
[19] G. Chen, Z. Tian, Y. Gong, Z. Chen, and J. A. Chambers, "Max-ratio relay selection in secure buffer-aided cooperative wireless networks," *IEEE Trans. Inf. Forensics and Security*, vol. 9, no. 4, pp. 719–729, Apr. 2014.
[20] H. Zhang, Y. Li, D. Jin, M. M. Hassan, A. Alelaiwi, and S. Chen, "Buffer-aided device-to-device communication: opportunities and challenges," *IEEE Commun. Mag.*, vol. 53, no. 12, pp. 67–74, Dec. 2015.
[21] G. Chen, Z. Tian, Y. Gong, and J. Chambers, "Decode-and-forward buffer-aided relay selection in cognitive relay networks," *IEEE Trans. Veh. Tech.*, vol. 63, no. 9, pp. 4723–4728, Nov. 2014.
[22] S. Luo and K. C. Teh, "Adaptive transmission for cooperative NOMA system with buffer-aided relaying," *IEEE Communications Letters*, vol. 21, pp. 937–940, Apr. 2017.
[23] Q. Zhang, Z. Liang, Q. Li, and J. Qin, "Buffer-aided non-orthogonal multiple access relaying systems in rayleigh fading channels," *IEEE Transactions on Communications*, vol. 65, pp. 95–106, Jan. 2017.
[24] R. Urgaonkar and M. J. Neely, "Delay-limited cooperative communication with reliability constraints in wireless networks," *IEEE Trans. Inf. Theory*, vol. 60, no. 3, pp. 1869–1882, Mar. 2014.
[25] I. Krikidis, T. Charalambous, and J. S. Thompson, "Buffer-aided relay selection for cooperative diversity systems without delay constraints," *IEEE Trans. Wireless Commun.*, vol. 11, no. 5, pp. 1957–1967, May 2012.
[26] S. Luo and K. C. Teh, "Buffer state based relay selection for buffer-aided cooperative relaying systems," *IEEE Trans. Wire. Commun.*, vol. 14, pp. 5430–5439, Nov. 2015.
[27] J. R. Norris, *Markov chains*. No. 2, Cambridge University Press, 1998.

Mohammad Alkhawatrah received the B.S. and M.S. degrees in communication engineering from Al-Ahliyya Amman University (AAU), Amman, Jordan, in 2008 and 2016, respectively. He is currently pursuing the Ph.D. degree with the Signal Processing and Networks Research Group in Wolfson School of Mechanical, Electrical and Manufacturing Engineering at Loughborough University, Loughborough, U.K. His research interests include buffer-aided relays, non-orthogonal multiple access, relay selection, cooperative networks.

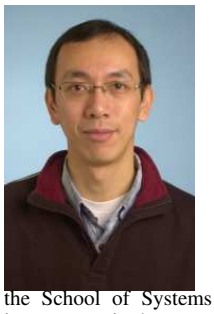

YuGong is with School of Electronic, Electrical and Systems Engineering, Loughborough University, UK, in July 2012. Dr Gong obtained his BEng and MEng in electronic engineering in 1992 and 1995 respectively, both at the University of Electronics and Science Technology of China. In 2002, he received his PhD in communications from the National University of Singapore. After PhD graduation, he took several research positions in Institute of Inforcomm Research in Singapore and Queens University of Belfast in the UK respectively. From 2006 and 2012, Dr Gong had been an academic member in the School of Systems Engineering, University of Reading, UK. His research interests are in the area of signal processing and communications including wireless communications, non-linear and non-stationary system identification and adaptive filters.

Gaojie Chen (S'09-M'12-SM'18) received the B.Eng. and B.Ec. degrees in electrical information engineering and international economics and trade from Northwest University, China, in 2006, and the M.Sc. (Hons.) and Ph.D. degrees in electrical and electronic engineering from Loughborough University, Loughborough, U.K., in 2008 and 2012, respectively. From 2008 to 2009, he was a Software Engineering with DTmobile, Beijing, China, and from 2012 to 2013, he was a Research Associate with the School of Electronic, Electrical and Systems Engineering, Loughborough University. He was a Research Fellow with 5GIC, Faculty of Engineering and Physical Sciences, University of Surrey, U.K., from 2014 to 2015. Then he was a Research Associate with the Department of Engineering Science, University of Oxford, U.K., from 2015 to 2018. He is currently a Lecturer with the Department of Engineering, University of Leicester, U.K. His research interests include information theory, wireless communications, IoT, cognitive radio, secrecy communication and random geometric networks. He received the Exemplary Reviewer Certificate of the IEEE WIRELESS COMMUNICATION LETTERS in 2018. He currently serves as an Editor of the IET ELECTRONICS LETTERS.

Sangarapillai Lambotharan (SM'06) received the Ph.D. degree in signal processing in 2017 from Imperial College London, London, where he remained until 1999 as a postdoctoral research associate. He was a visiting scientist with the Engineering and Theory Centre of Cornell University, USA in 1996. He is a Professor of Digital Communications and the Head of Signal Processing and Networks Research Group with the Wolfson School Mechanical, Electrical and Manufacturing Engineering, Loughborough University, Loughborough, U.K. Between 1999 and 2002, he was with Motorola Applied Research Group, U.K. and investigated various projects including physical link layer modeling and performance characterization of GPRS, EGPRS, and UTRAN. He was with Kings College London and Cardiff University as a Lecturer and Senior Lecturer, respectively, from 2002 to 2007. His current research interests include 5G networks, MIMO, radars, smart grids, machine learning, network security, and blockchain technology. He has authored more than 200 journal and conference articles in these areas.

Jonathon Chambers (S'83-M'90-SM'98-F'11) received the Ph.D. and D.Sc. degrees in signal processing from Imperial College London, London, U.K., in 1990 and 2014, respectively. From 1991 to 1994, he was a Research Scientist with the Schlumberger Cambridge Research Center, Cambridge, U.K. In 1994, he returned to Imperial College London as a Lecturer in signal processing and was promoted to a Reader (Associate Professor) in 1998. From 2001 to 2004, he was the Director of the Center for Digital Signal Processing and a Professor of signal processing with the Division of Engineering, Kings College London, where he is currently a Visiting Professor. From 2004 to 2007, he was a Cardiff Professorial Research Fellow with the School of Engineering, Cardiff University, Cardiff, U.K. From 2007 to 2014, he led the Advanced Signal Processing Group, School of Electronic, Electrical and Systems Engineering, Loughborough University, where he is also a Visiting Professor. In 2015, he joined the School of Electrical and Electronic Engineering, and he has been with the School of Engineering, Newcastle University, Newcastle upon Tyne, U.K., since 2017. Since 2017, he has also been a Professor in engineering and the Head of Department, University of Leicester, Leicester, U.K. He is also the International Honorary Dean and a Guest Professor with the Department of Automation, Harbin Engineering University, Harbin, China. He has advised almost 80 researchers through to Ph.D. graduation and has published over 500 conference proceedings and journal articles, many of which are in IEEE journals. His research interests include adaptive signal processing and machine learning and their application in communications, defence, and navigation systems.

Dr. Chambers is a fellow of the Royal Academy of Engineering, U.K., the Institution of Engineering and Technology, and the Institute of Mathematics and its Applications. He was a Technical Program Co-Chair of the 36th IEEE International Conference on Acoustics, Speech, and Signal Processing (ICASSP), Prague, Czech Republic. He is serving on the Organizing Committees of ICASSP 2019, Brighton, U.K., and ICASSP 2022, Singapore. He has served on the IEEE Signal Processing Theory and Methods Technical Committee for six years, the IEEE Signal Processing Society Awards Board for three years, and the Jack Kilby Medal Committee for three year. He was an Associate Editor of the IEEE Transactions on Signal Processing for three terms over the periods 1997-1999, 2004-2007, and a Senior Area Editor from 2011 to 2015.